PERGAMON

International Journal of Heat and Mass Transfer 42 (1999) 3373–3385

International Journal of HEAT and MASS TRANSFER

On departure from local thermal equilibrium in porous media due to a rapidly changing heat source: the Sparrow number

W.J. Minkowycz[a], A. Haji-Sheikh[b,*], K. Vafai[c]

[a]*Department of Mechanical Engineering, University of Illinois at Chicago, Chicago, IL 60607-7022, USA*
[b]*Department of Mechanical and Aerospace Engineering, The University of Texas at Arlington, Arlington, TX 76019-0023, USA*
[c]*Department of Mechanical Engineering, The Ohio State University, Columbus, OH 43210-1107, USA*

Received 10 October 1998; received in revised form 15 January 1999

Abstract

Local thermal equilibrium is an often-used hypothesis when studying heat transfer in porous media. Examination of non-equilibrium phenomena shows that this hypothesis is usually not valid during rapid heating or cooling. The results from this theoretical study confirm that local thermal equilibrium in a fluidized bed depends on the size of the layer, mean pore size, interstitial heat transfer coefficient, and thermophysical properties. For a porous medium subject to rapid transient heating, the existence of the local thermal equilibrium depends on the magnitude of the Sparrow number and on the rate of change of the heat input.

1. Introduction

Flow and heat transfer in porous media have broad applications in engineering practice. They extend over a wide range of applications such as in geological [1–3], food processing [4,5], building insulation and infiltration [6–9], nuclear reactor design [10,11], nuclear waste processing [12], fundamental flow, and heat and mass transfer research [13–30]. Summaries of earlier work are included in monograms and books [31–34]. In general, various analytical studies used in dealing with flow and heat transfer in porous media hypothesize the existence of local thermal equilibrium (LTE); that is, the solid and the neighboring liquid are at the same temperature. This paper establishes conditions when early departure from local thermal equilibrium occurs in the presence of a rapidly changing volumetric heat source or surface heat flux.

In the absence of local thermal equilibrium, the single energy equation needs to be replaced with two energy equations, one for the solid and another for the fluid. Investigations by Vafai and Sozen [35], which were based on the two-phase equation model, reported significant discrepancies between the fluid and the solid phase temperature distributions. Later Amiri and Vafai [36,37] investigated the validity of local thermal equilibrium (LTE) conditions for steady state as well as transient incompressible flow through a porous medium. Also, in Lee and Vafai [38], a theoretical investigation of forced convective flow through a channel filled with a porous medium was presented. In their work, conceptual assessment and an analytical characterization of fluid and solid temperature differentials as well as the breakdown of the LTE assumption were established.

* Corresponding author. Tel.: +1 817 272 2010; fax: +1 817 272 2952.
E-mail address: haji@mae.uta.edu (A. Haji-Sheikh)

0017-9310/99/$ - see front matter
PII: S0017-9310(99)00043-5

Nomenclature

a_c	parameter in Refs. [36,37]
a_m	$\gamma_m - \beta_m$
A_p	pore surface area, m^2
C	$\epsilon C_\mathrm{f} + (1-\epsilon)C_\mathrm{s}$
$\bar{C}$	$(1-\epsilon)C_\mathrm{s}/C$
C_f	fluid heat capacitance, $\mathrm{J\ m^{-3}\ K^{-1}}$
C_s	solid heat capacitance, $\mathrm{J\ m^{-3}\ K^{-1}}$
$F_n(\boldsymbol{r})$	eigenfunction
Fo	Fourier number, $k_e t/CL^2$
h	interstitial heat transfer coefficient, $\mathrm{W\ m^{-2}\ K^{-1}}$
k_e	equivalent thermal conductivity, $\mathrm{W\ m^{-1}\ K^{-1}}$
$\bar{L}$	$C_\mathrm{f} u_0 L/k_e$
L	porous layer thickness, m
$\mathscr{L}$	operator, $\nabla\cdot(k_e\nabla) - C_\mathrm{f}\mathbf{V}\cdot\nabla$
m, n	indices
N_n	norms
Pe	Peclet number, $\lvert\bar{L}\rvert$
q	heat flux, $\mathrm{W\ m^{-2}}$
q_0	heat flux amplitude, $\mathrm{W\ m^{-2}}$
r_h	hydraulic radius, $\Delta V_\mathrm{p}/\Delta A_\mathrm{p}$, as defined after Eq. (2), m
R_c	contact resistance, $\mathrm{m^2\ K\ W^{-1}}$
S	volumetric heat source, $\mathrm{W\ m^{-3}}$
S_n^*	see Eq. (15)
Sp	Sparrow number, $hL^2/k_e r_\mathrm{h}$
t	time, s
$\bar{t}$	$Fo(Pe)^2$
T	temperature, K
u_0	mean velocity, $\mathrm{m\ s^{-1}}$
$\mathbf{V}$	velocity vector
V	volume, $\mathrm{m^3}$
x	coordinate, m
$\bar{x}$	$C_\mathrm{f} u_0 x/k_e$
$w(\boldsymbol{r})$	weighting function.

Greek symbols

α	thermal diffusivity, $\mathrm{m^2\ s^{-1}}$
β_n	parameter related to γ_n, Eq. (13)
γ_n	eigenvalue
ϵ	V_f/V
λ_n	parameter related to γ_n, Eq. (14)
ν	$2\pi \times$ frequency, $\mathrm{rad\ s^{-1}}$
τ	dummy variable and Green's function parameter
τ_e	$(1-\epsilon)C_\mathrm{s}\tau_t/C$, s
τ_q	lag time, heat flux, s
τ_t	lag time, $\tau_t \approx r_\mathrm{h} C_\mathrm{f}/h$, s
ω_n	see Eq. (17).

Subscripts

f	fluid
p	pore
s	solid.

This paper presents a modified energy equation that can be solved for very early departures from LTE conditions while assuming the velocity field is known from the solution of continuity and momentum equation. A numerical solution requires the knowledge of a new set of parameters. Clearly, there is a paucity of needed information for in-depth evaluation of this departure from the local thermal equilibrium phenomena. In this paper, the emphasis is on the demonstration of the underlying physical phenomena for an early departure from LTE conditions. To this end, this work considers a simplified flow model.

Parametric studies reported here describe the role of a dimensionless quantity that identifies the early departure from local thermal equilibrium in the presence of a rapidly changing heat source. The numerically obtained data reveal the implication of nonequilibrium thermal phenomena in a fluid-saturated porous medium in the presence of a volumetric heat source. In this work, early departure from the local thermal equilibrium in applications where there is a rapid change in the surface heat flux, e.g., in combustors and in laser heating applications, is analyzed.

2. Theoretical model

The concept of local thermal equilibrium is widely used in the majority of heat transfer applications involving porous media. An in-depth analysis of non-thermal equilibrium is reported by Amiri and Vafai [36,37] for both steady state and transient conditions. Also, in their work the impact of dispersion and non-Darcian effects on LTE is analyzed. A study of LTE for compressible fluid flow is presented in Vafai and Sozen [35]. Their results indicate that the Darcy number and the particle Reynolds number are influential parameters in determining the validity of local thermal equilibrium. In these works, Vafai and coworkers consider the solid and fluid as two independent systems that exchange energy by convection at the local porous fluid interface. This paper investigates the conditions when there is a relatively small departure from local thermal equilibrium due to rapid transient heating. This non-equilibrium phenomenon occurs depending on the nature of the transient heat source, ratio of the characteristic length to pore size, velocity field, and the thermophysical properties of the medium. These variables can be cast into a set of dimensionless groups that will emerge through analysis presented later in this work. They will be used as a guide to indicate whether the LTE condition exists or the solid and fluid should be treated as different systems.

2.1. Energy equation

When the thermophysical properties are independent of temperature and flow is incompressible, the continuity and momentum equation [36,37] yield the velocity distribution. Next, consideration is given to a differential element in the flow field that contains both solid and fluid phases. The energy equation applied to a control volume under a locally non-equilibrium thermal condition leads to the following set of governing equations [36,37]:

$$\epsilon C_{\mathrm{f}}\frac{\partial T_{\mathrm{f}}(\boldsymbol{r},t)}{\partial t}+C_{\mathrm{f}}\mathbf{V}\cdot\nabla T_{\mathrm{f}} =-\nabla\cdot\boldsymbol{q}_{\mathrm{f}}(\boldsymbol{r},t)+hA_{\mathrm{p}}a_c(T_{\mathrm{s}}-T_{\mathrm{f}}) \tag{1a}$$

$$(1-\epsilon)C_{\mathrm{s}}\frac{\partial T_{\mathrm{s}}(\boldsymbol{r},t)}{\partial t}=-\nabla\cdot\boldsymbol{q}_{\mathrm{s}}(\boldsymbol{r},t)-hA_{\mathrm{p}}a_c(T_{\mathrm{s}}-T_{\mathrm{f}}) \tag{1b}$$

Adding Eqs. (1a) and (b), replacing $\boldsymbol{q}_{\mathrm{f}}+\boldsymbol{q}_{\mathrm{s}}$ with $\boldsymbol{q}$, and including the contribution of a volumetric heat source, $S(\boldsymbol{r},t)$, yields the relation

$$-\nabla\cdot\boldsymbol{q}(\boldsymbol{r},t)+S(\boldsymbol{r},t) =\epsilon C_{\mathrm{f}}\frac{\partial T_{\mathrm{f}}(\boldsymbol{r},t)}{\partial t}+C_{\mathrm{f}}\mathbf{V}\cdot\nabla T_{\mathrm{f}}+(1-\epsilon)C_{\mathrm{s}}\frac{\partial T_{\mathrm{s}}(\boldsymbol{r},t)}{\partial t} \tag{1c}$$

where $\epsilon=V_{\mathrm{f}}/V$ is the fraction of the volume the fluid occupies. Under a local thermal equilibrium condition, it is assumed that the solid and the adjacent fluid are at the same temperature, $T_{\mathrm{s}}=T_{\mathrm{f}}$. Under a rapid heating condition, which is analyzed in this work, the fluid and solid are not at the same temperature at a local level. It is hypothesized that, before the onset of equilibrium, the fluid temperature undergoes a transient process defined by the relation

$$C_{\mathrm{f}}\Delta V_{\mathrm{p}}\frac{\partial T_{\mathrm{f}}}{\partial t}=h\Delta A_{\mathrm{p}}(T_{\mathrm{s}}-T_{\mathrm{f}}) \tag{2}$$

where ΔV_{p} and ΔA_{p} are volume and surface area of a mean pore, and h is the interstitial heat transfer coefficient. As a shorthand notation, let $r_{\mathrm{h}}=\Delta V_{\mathrm{p}}/\Delta A_{\mathrm{p}}$, where r_{h} can be considered to be a pore hydraulic radius. Eq. (2) can then be stated as

$$T_{\mathrm{s}}(\boldsymbol{r},t)=T_{\mathrm{f}}(\boldsymbol{r},t)+\frac{r_{\mathrm{h}}C_{\mathrm{f}}}{h}\frac{\partial T_{\mathrm{f}}(\boldsymbol{r},t)}{\partial t} \tag{3}$$

Under a local thermal equilibrium condition, $T_{\mathrm{f}}=T_{\mathrm{s}}$, and the Fourier equation is

$$\boldsymbol{q}(\boldsymbol{r},t)=-k_e\nabla T_{\mathrm{f}}(\boldsymbol{r},t) \tag{4}$$

where k_e is the equivalent thermal conductivity of the porous medium. It is reported that under a rapid heating process, e.g., by Fournier and Boccara [39], Eq. (4)

does not hold. A comprehensive literature survey of earlier work is in Ref. [37]. In the absence of local equilibrium, when the departures of $\boldsymbol{q}$ and ∇T from local equilibrium are small, it is suggested in Ref. [40] that the Fourier equation, as given in Eq. (4), needs to be modified to

$$\boldsymbol{q}(\boldsymbol{r},t)+\Delta\boldsymbol{q}(\boldsymbol{r},t)=-k_e\{\nabla T_{\rm f}(\boldsymbol{r},t)+\Delta[\nabla T_{\rm f}(\boldsymbol{r},t)]\} \tag{5}$$

Since the differential changes on both sides of Eq. (5) are time dependent, Eq. (5) can be written as

$$\boldsymbol{q}(\boldsymbol{r},t)+\tau_q\frac{\partial\boldsymbol{q}(\boldsymbol{r},t)}{\partial t}=-k_e\left\{\nabla T_{\rm f}(\boldsymbol{r},t)+\tau_t\frac{\partial}{\partial t}[\nabla T_{\rm f}(\boldsymbol{r},t)]\right\} \tag{6}$$

According to Eq. (3), the relaxation time τ_t is approximated by $\tau_t\approx r_{\rm h}C_{\rm f}/h$. Based on the physical reasoning, one can hypothesize that $\tau_q\approx C_{\rm s}R_{\rm c}\Delta V_{\rm s}/\Delta A_{\rm s}$, where $\Delta V_{\rm s}$ is the volume of a solid structure while $R_{\rm c}$ and $\Delta A_{\rm s}$ are the contact resistance and contact area between individual solid structures, respectively. The derivation of this approximate relation for τ_q is in a later section.

One can use Eqs. (3) and (6) to eliminate $T_{\rm s}$ and $\boldsymbol{q}$ in Eq. (1c), resulting in

$$\begin{aligned}&\mathscr{L}(T_{\rm f})+\tau_q\frac{\partial}{\partial t}[\mathscr{L}(T_{\rm f})]+(\tau_t-\tau_q)\frac{\partial[\nabla\cdot(k_e\nabla T_{\rm f})]}{\partial t}\\&+\left(S+\tau_q\frac{\partial S}{\partial t}\right)\\&=C\frac{\partial}{\partial t}\left[T_{\rm f}+(\tau_e+\tau_q)\frac{\partial T_{\rm f}}{\partial t}+\tau_e\tau_q\frac{\partial^2T_{\rm f}}{\partial t^2}\right]\end{aligned} \tag{7}$$

where $T_{\rm f}=T_{\rm f}(\boldsymbol{r},\ t)$, $S=S(\boldsymbol{r},\ t)$, $\mathscr{L}(T_{\rm f})=\nabla\cdot(k_e\nabla T_{\rm f})-C_{\rm f}\mathbf{V}\cdot\nabla T_{\rm f}$, $C=\epsilon C_{\rm f}+(1-\epsilon)C_{\rm s}$, and $\tau_e=(1-\epsilon)C_{\rm s}\tau_t/C$. Since $\tau_e\tau_q<(\tau_e+\tau_q)^2/2!$, the third-order derivative on the right-hand-side of Eq. (7) is small and can be neglected. This is consistent with earlier derivations where the terms of the second-order in Eqs. (3) and (6) are neglected; therefore, this approximation reduces Eq. (7) to

$$\begin{aligned}&\mathscr{L}(T_{\rm f})+\tau_q\frac{\partial}{\partial t}[\mathscr{L}(T_{\rm f})]+(\tau_t-\tau_q)\frac{\partial[\nabla\cdot(k_e\nabla T_{\rm f})]}{\partial t}\\&+\left(S+\tau_q\frac{\partial S}{\partial t}\right)\\&=C\left[\frac{\partial T_{\rm f}}{\partial t}+(\tau_e+\tau_q)\frac{\partial^2T_{\rm f}}{\partial t^2}\right]\end{aligned} \tag{8}$$

For a few special cases, Eq. (8) has an exact solution; however, in general, the solution requires a numerical procedure. One special case is the study of the temperature field in a porous medium when $\mathbf{V}=0$. In this case, Eq. (8), without the term $C_{\rm f}\mathbf{V}\cdot\nabla T_{\rm f}$, is similar to the thermal conduction equation for energy exchange in microscale systems. Therefore, the solution of Eq. (8) for no-flow or negligible flow rate, as given in Ref. [41], is

$$T_{\rm f}(\boldsymbol{r},t)=T_{\rm I}(\boldsymbol{r},t)+T_{\rm S}(\boldsymbol{r},t) \tag{9}$$

where the solution given in Eq. (9) is composed of two parts, the contribution from the initial condition, $T_{\rm I}$, and the contribution from the volumetric heat source, $T_{\rm S}$. It should be noted that $T_{\rm S}$ may also contain the contribution of the nonhomogeneous boundary conditions. The contribution from the initial condition is

$$\begin{aligned}T_{\rm I}(\boldsymbol{r},t)=\sum_{n=1}^{\infty}\frac{F_n(\boldsymbol{r})}{N_n}{\rm e}^{-(\gamma_n-\beta_n)t}&\left\{\frac{\sinh[\sqrt{(\beta_n^2-\lambda_n^2)}t]}{\sqrt{(\beta_n^2-\lambda_n^2)}}\right.\\&\times\left[(\gamma_n-\beta_n)\int_V F_n(\boldsymbol{r}')T_i(\boldsymbol{r}')\,{\rm d}V'\right.\\&\left.\left.+\int_V F_n(\boldsymbol{r}')T_{ii}(\boldsymbol{r}')\,{\rm d}V'\right]\right.\\&\left.+\cosh[\sqrt{(\beta_n^2-\lambda_n^2)}t]\int_V F_n(\boldsymbol{r}')T_i(\boldsymbol{r}')\,{\rm d}V'\right\}\end{aligned} \tag{10}$$

where $T_i(\boldsymbol{r})$ and $T_{ii}(\boldsymbol{r})$ are the temperature and the time derivative of temperature at $t=0$. The contribution of the volumetric heat source is

$$\begin{aligned}T_{\rm S}(\boldsymbol{r},t)=\sum_{n=1}^{\infty}\int_{\tau=0}^{t}\int_V&\left(\frac{F_n(\boldsymbol{r})F_n(\boldsymbol{r}')}{CN_n}\right){\rm e}^{-\gamma_n(t-\tau)}\\&\times\left\{\frac{{\rm e}^{\beta_n(t-\tau)}\sinh[\sqrt{(\beta_n^2-\lambda_n^2)}(t-\tau)]}{(\tau_q+\tau_e)\sqrt{(\beta_n^2-\lambda_n^2)}}\right\}\\&\times\left(S(\boldsymbol{r}',\tau)+\tau_q\frac{\partial S(\boldsymbol{r}',\tau)}{\partial\tau}\right){\rm d}V'\,{\rm d}\tau\end{aligned} \tag{11}$$

In Eqs. (10) and (11), the eigenfunction $F_n(\boldsymbol{r})$ is the solution of equation

$$\nabla\cdot[k_e\nabla F_n(\boldsymbol{r})]=-\gamma_nCF_n(\boldsymbol{r}) \tag{12a}$$

and N_n is the norm

$$N_n=\int_V w(\boldsymbol{r})[F_n(\boldsymbol{r})]^2\,{\rm d}V \tag{12b}$$

with a weighting function $w(\boldsymbol{r})$. The symbols β_n, λ_n, and $S_n^*(t)$ are shorthand notations defined by the relations

$$\beta_n = \gamma_n\left[1 - \frac{1}{2}\,\frac{\tau_t}{\tau_q+\tau_e} - \frac{1}{2\gamma_n(\tau_q+\tau_e)}\right] \tag{13}$$

$$\lambda_n = \gamma_n\left[1 - \frac{\tau_t}{\tau_q+\tau_e}\right]^{1/2} \tag{14}$$

$$S_n^*(t) = \frac{e^{\gamma_n t}}{N_n C(\tau_q+\tau_e)}$$

$$\int_V w(\boldsymbol{r})F_n(\boldsymbol{r})\left(S(\boldsymbol{r},t) + \tau_q\frac{\partial S(\boldsymbol{r},t)}{\partial t}\right)\mathrm{d}V \tag{15}$$

Eqs. (10) and (11) are cast in the form of Green's function solution in [41], and they are derived when $\mathbf{V}=0$. In general, when velocity is finite, the computation of temperature requires a numerical scheme. However, Eqs. (10) and (11) can also be used in the presence of a flow when $\mathbf{V}=$constant with an additional restriction, that is, $\tau_q=\tau_t$. For this specific case, $F_n(\boldsymbol{r})$ in Eqs. (10), (11), and (12b) is the solution of equation

$$\mathscr{L}[F_n(\boldsymbol{r})] = -\gamma_n C F_n(\boldsymbol{r}) \tag{16}$$

instead of Eq. (12a).

3. Results

The temperature solution and relevant steps will be demonstrated through two numerical examples. Example 1 considers a porous layer with no through flow, Fig. 1a. In the presence of a flow, Fig. 1b, as discussed in Example 2, major modifications of the solution technique are necessary. The examples will identify both the required conditions for the local thermal equilibrium and the effect of departure from the equilibrium condition.

3.1. Example 1. Conduction solution

To study the parameters that govern the local thermal equilibrium condition, a porous plate with thickness L is examined, as shown in Fig. 1a. The plate is insulated on one side, $x=L$, and the other side, at $x=0$, is subject to a periodic surface heat flux, and there is no flow through the porous slab. This porous slab is initially at a uniform temperature so that $T_i=T_{ii}=0$. Now, one can simulate different periodic heat inputs by studying the effects of harmonically varying heat inputs. This is a systematic method of studying the effect of heat flux for various functional forms since any such function can be decomposed into a series of sines and cosines using the Fourier series, or

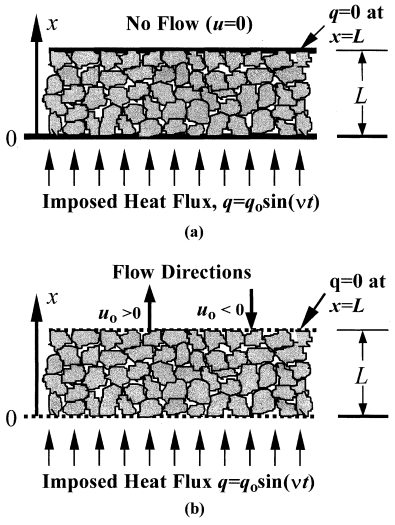

Fig. 1. Schematic of a fluid-saturated porous medium; (a) no flow, (b) with flow.

using the Fourier integral. It should be noted that the evaluation of the effective conductivity is in itself an important problem as discussed in detail in Tien and Vafia [42].

Therefore, the volumetric heat source S is taken as $S=\delta(x-0)q_0\sin(\nu t)$ in Eq. (11), where the Dirac delta function $\delta(x-0)=1$ when $x=0$, otherwise $\delta(x-0)=0$. The eigenfunctions of Eq. (12a) for the above-mentioned boundary conditions are $\cos(m\pi x/L)$ that yield the eigenvalues $\gamma_m=(m\pi/L)^2k_e/C$ for $m=0,\ 1,\ 2,\ldots,$. The temperature solution of Eq. (11), retaining τ_q, τ_t, and τ_e, and defining the parameters $a_m=\gamma_m-\beta_m$, $\gamma_m=(m\pi/L)^2k_e/C$, and $\omega_m=(\beta_m^2-\lambda_m^2)^{1/2}$ is

$$\begin{aligned}\frac{k_eT_f}{q_0L} = \sum_{m=0}^{\infty}\frac{LF_m(x)}{N_m\omega_m(\tau_e+\tau_q)}\{&(\Lambda_1+\nu\tau_q\Lambda_2)\\ &\times\exp[-a_mk_et/(CL^2)] + (\Gamma_{s1}+\nu\tau_q\Gamma_{s2})\\ &\times\sin(\nu t) + (\Gamma_{c1}+\nu\tau_q\Gamma_{c2})\cos(\nu t)\}/\\ &[\nu^4+(a_m^2-\omega_m^2)^2+2\nu^2(a_m^2+\omega_m^2)]\end{aligned} \tag{17}$$

wherein the eigenfunction is $F_m(x)=\cos(m\pi x/L)$ and the norm is $N_m=L$ when $m=0$ and $N_m=L/2$ when $m>0$. Other parameters appearing in Eq. (17) are:

$$\begin{aligned}\Lambda_1 = \nu[&2a_m\omega_m\cosh(\omega_mt)\\ &+(\nu^2+a_m^2+\omega_m^2)\sinh(\omega_mt)]\end{aligned} \tag{18a}$$

$$\begin{aligned}\Lambda_2 = [&\omega_m(\nu^2-a_m^2+\omega_m^2)\cosh(\omega_mt)\\ &-(\nu^2+a_m^2-\omega_m^2)\sinh(\omega_mt)]\end{aligned} \tag{18b}$$

$$\Gamma_{s1} = \Gamma_{c2} = -\omega_m(\nu^2 - a_m^2 + \omega_m^2)$$
$$\text{and} \quad \Gamma_{c1} = -\Gamma_{s2} = -2\nu a_m \omega_m \tag{18c}$$

This parametric study considers two limiting cases. The first limiting case, corresponding to $\tau_q = 0$, shows a relatively larger departure from the LTE condition, that is, a small τ_q enhances the nonequilibrium transient behavior of a system. The second limiting case, for $\tau_q = \tau_t$, produces a relatively smaller departure from LTE for most of the frequencies.

An observation of the governing equations shows that the local thermal equilibrium holds when $C_f r_h/h$ is small. When time t is cast in dimensionless form as $Fo = k_e t/CL^2$, the other dimensionless parameters that control the state of local thermal equilibrium are C_s/C and $Sp = hL^2/k_e r_h$. The surface heat flux in terms of dimensionless parameters is $q_0 \sin[(\nu CL^2/k_e)Fo]$, where $\nu CL^2/k_e$ is the dimensionless frequency. The dimensionless quantity Sp contains the contributions of the flow in porous media, interstitial heat transfer, and general thermal conduction. It is proposed that it be called the Sparrow number because of numerous pioneering contributions of Professor E. M. Sparrow to a broad range of heat transfer topics including porous media. The following numerical results show that the local thermal equilibrium, $T_f \cong T_s$, exists when Sp is large.

The solution, using Eq. (17), describes the parametric behavior of the system. The dimensionless solid and fluid temperatures are calculated as a function of the Fourier number, for $\nu CL^2/k_e = 10$, and $Sp = 10$. The results are plotted in Fig. 2a for $x = 0$ and in Fig. 2b for $x = L$. The data clearly show the difference between solid and fluid temperatures due to the nonequilibrium thermal behavior of the flow. Also, the data in the figures show that the dimensionless quantity, $\bar{C} = (1-\epsilon)C_s/C$, influences the temperature values. There is a relatively larger spreading of temperature data in Fig. 2b than in Fig. 2a. The computation is repeated using $Sp = 100$ and the results are shown in Figs. 3a and b. The data in Fig. 3a, for $x = 0$, show a near thermal equilibrium condition, that is, $T_f \cong T_s$. Also, Fig. 3b shows a similar behavior indicating the existence of near local thermal equilibrium throughout the porous medium, and the influence of the variations in the parameter $\bar{C}$ is substantially diminished. Accordingly, for most practical applications, the local thermal equilibrium is satisfied when $Sp > 100$; however, for very fast transients, Sp should be as much as 500 or more. The next set of data demonstrates this effect.

To show the effect of slowly and rapidly changing surface heat flux, the periodic terms in Eq. (17) are cast in the form $\sin(\nu t - \phi)$ where ϕ is the phase angle. The phase angle and the amplitude can be considered

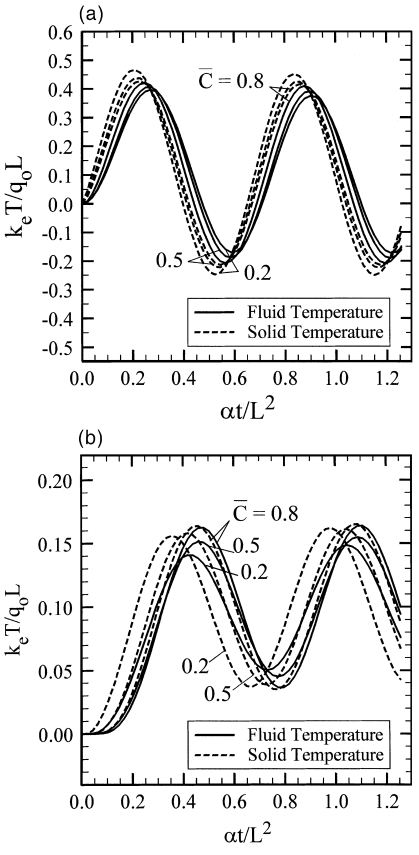

Fig. 2. (a) Fluid and solid temperature at $x = 0$ when $q(0, t) = q_0 \sin(\nu t)$, $Sp = 10$, $u_0 = 0$, $\tau_q = 0$, and $\nu CL^2/k_e = 10$. (b) Fluid and solid temperature at $x = L$ when $q(0, t) = q_0 \sin(\nu t)$, $Sp = 10$, $u_0 = 0$, $\tau_q = 0$, and $\nu CL^2/k_e = 10$.

as indicators of the thermal performance of a porous layer subject to a rapidly changing heating condition. Fig. 4a shows the computed values of the phase angle and Fig. 4b describes the amplitude at $x = L$. The data are plotted for $Sp = 10$, 50, and 100 and for three specific heat ratios, $\bar{C} = 0.2$, 0.5, and 0.8. Fig. 4a shows that for high frequency surface heat flux, especially when $\bar{C}$ is small, much higher values of the Sparrow number are needed to achieve the condition of local thermal equilibrium. According to Fig. 4b, the amplitudes behave nearly the same as those for the local thermal equilibrium except for the $Sp = 10$ line when $\bar{C} = 0.2$. The logarithmic scale in Fig. 4b enables one to observe small departures from the LTE condition. The solid lines, designated as $Sp = \infty$ in Figs. 4a and b, are solutions in the presence of the LTE condition.

Numerical data are collected to show the limiting performance of this solution when $\tau_q = \tau_t$. This is a favorable condition for occurrence of the local thermal equilibrium condition. Prior to examining the numerical data, this limiting tendency is apparent after

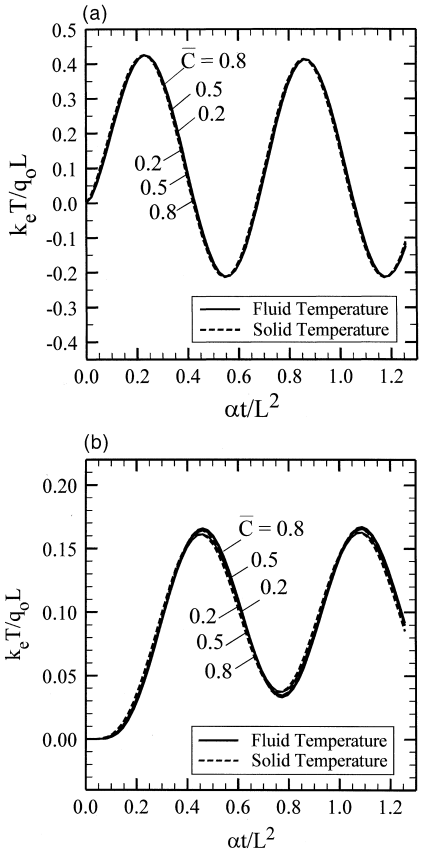

Fig. 3. (a) Fluid and solid temperature at $x=0$ when $q(0,\ t)=q_0\ \sin(\nu t)$, $Sp=100$, $u_0=0$, $\tau_q=0$, and $\nu CL^2/k_e=10$. (b) Fluid and solid temperature at $x=L$ when $q(0,\ t)=q_0\ \sin(\nu t)$, $Sp=100$, $u_0=0$, $\tau_q=0$, and $\nu CL^2/k_e=10$.

rewriting Eq. (8) as

$$\left[\mathscr{L}(T_{\mathrm{f}})+S-C\frac{\partial T_{\mathrm{f}}}{\partial t}\right] + \tau_q\frac{\partial}{\partial t}\left[\mathscr{L}(T_{\mathrm{f}})+S-C\frac{\partial T_{\mathrm{f}}}{\partial t}\right] = (\tau_t-\tau_q)\frac{\partial[\nabla\cdot(k_e\nabla T_{\mathrm{f}})]}{\partial t}+\tau_t\bar{C}\frac{\partial^2 T_{\mathrm{f}}}{\partial t^2} \tag{19a}$$

When $\tau_q=\tau_t$, the first term on the right-hand-side of Eq. (19a) vanishes. For this special case, the equilibrium solution satisfies equation

$$\mathscr{L}(T_{\mathrm{f}})+S-C\frac{\partial T_{\mathrm{f}}}{\partial t}=0 \tag{19b}$$

and it will satisfy Eq. (19a) if $\bar{C}=(1-\epsilon)C_{\mathrm{s}}/C\rightarrow 0$ because both remaining terms in the square brackets, Eq. (19a), contain the left-hand-side of Eq. (19b). In general, the solution of Eq. (19a), when $\tau_q=\tau_t$, shows

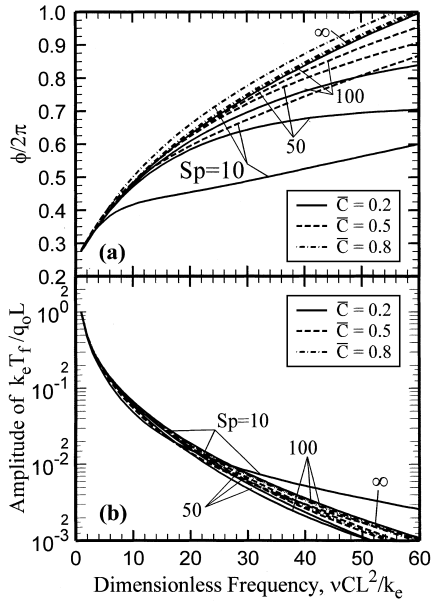

Fig. 4. Variation (a) phase angle (b) amplitude with dimensionless frequency, $\nu CL^2/k_e$, at $x=L$ when $\tau_q=0$ and $u_0=0$ for different Sparrow numbers, Sp.

the departure from the local thermal equilibrium condition due to the influence of the term $\tau_t\bar{C}\ \partial^2 T_{\mathrm{f}}/\partial t^2$. The computed phase angles and amplitudes at $x=L$ for heat flux inputs of different frequency, in Figs. 5a and b, show this tendency.

The phase angles shown in Fig. 5a have generally higher phase angles than those in Fig. 4a. The phase angles, when $Sp=100$, have nearly the same phase angles as those for the local thermal equilibrium values up to the dimensionless frequency of 15. For higher frequency heat inputs, the deviations from the local thermal equilibrium solutions are smaller than those shown in Fig. 4a. Furthermore, the amplitudes plotted in Fig. 5b are approximately the same as those for the LTE solution when $\nu CL^2/k_e<15$. This implies that when $\tau_q=\tau_t$ and $Sp>100$, the condition of the local thermal equilibrium is satisfied for all practical applications. A comparison between Figs. 4a–b and Figs. 5a–b shows that, for a given Sparrow number, it is more likely to approach LTE as τ_q approaches τ_t.

3.2. Example 2. Uniform-flow solution

To demonstrate the differences between this solution and the solution in Example 1, it is assumed that there is a given heat flux at $x=0$ and the surface at $x=L$ is insulated. There is a flow with a constant mean velocity u_0 in the x- or opposite to the x-direction. For this example, it is assumed that $\tau_q=\tau_t$ for two reasons: (1) the availability of an exact solution for this case, and (2) this is a favorable condition for occurrence of

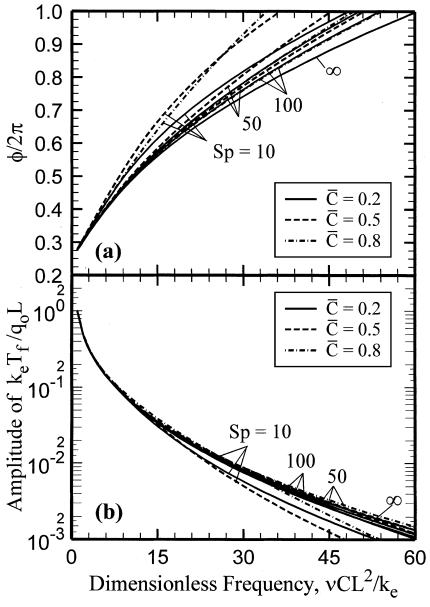

Fig. 5. Variation (a) phase angle (b) amplitude with dimensionless frequency, $\nu CL^2/k_e$, at $x=L$ when $\tau_q=\tau_t$ and $u_0=0$ for different Sparrow numbers, *Sp*.

the local thermal equilibrium. For this specific case, other boundary conditions can be accommodated by the classical approach. Accordingly, Eq. (17) can provide a solution to this problem following other modifications described below.

Consideration is given to finding the temperature field when a fluid with velocity u_0 is passing through a porous medium along the x-direction. Preliminary to finding such a solution, it is essential to find a particular solution of the equation

$$k_e\frac{\partial^2\theta}{\partial x^2}-C_{\mathrm{f}}u_0\frac{\partial\theta}{\partial x}=C\frac{\partial\theta}{\partial t} \tag{20}$$

This is a classical one-dimensional conduction in a moving body whose solution is readily available, see [43], p. 69. A schematic of the porous medium set-up corresponding to this case is shown in Fig. 1b. If a fluid flows in the opposite direction of the coordinate x, then u_0 is negative. When the independent variables are cast in the dimensionless form, this equation becomes

$$\frac{\partial^2\theta}{\partial\bar{x}^2}-\frac{\partial\theta}{\partial\bar{x}}=\frac{\partial\theta}{\partial\bar{t}} \tag{21}$$

where

$$\bar{x}=C_{\mathrm{f}}u_0x/k_e \tag{22a}$$

and

$$\bar{t}=C_{\mathrm{f}}^2u_0^2t/Ck_e=(k_et/CL^2)(C_{\mathrm{f}}u_0L/k_e)$$
$$=Fo(Pe)^2 \tag{22b}$$

The Peclet number $Pe=C_{\mathrm{f}}|u_0|L/k_e$ and the Fourier number $Fo=k_et/CL^2$ are based on the mean thermal conductivity value. The eigenfunctions and eigenvalues for this partial differential equation are

$$F_m(\bar{x})=1-\bar{x}/2 \quad \text{when } m=0 \tag{23a}$$

$$F_m(\bar{x})=[\cos(m\pi\bar{x}/\bar{L})-\bar{L}\,\sin(m\pi\bar{x}/\bar{L})/2m\pi \,]\exp(\bar{x}/2) \tag{23b}$$

$$\text{for } m=1,2,\ldots,\infty$$

and

$$\gamma_m=(m\pi/\bar{L})^2+1/4 \quad \text{for } m=0,1,2,\ldots,\infty \tag{23c}$$

where $|\bar{L}|=Pe$. The particular solution to be used to construct the general solution is

$$\theta=\sum_{m=0}^{\infty}\psi_m[\cos(m\pi x/L)-\frac{\bar{L}}{2m\pi}\sin(m\pi x/L)]\,\mathrm{e}^{\bar{x}/2}\,\mathrm{e}^{-\gamma_m\bar{t}} \tag{24}$$

Therefore, it is possible to compute the temperature distribution from Eq. (17) after replacing the eigenfunctions by Eqs. (23a, b), the eigenvalues by Eq. (23c), and by a new value for the norm. The new value of the norm for inclusion in Eq. (17) is calculated using the weighting function $w(x)=\exp(-\bar{x})$ and Eq. (12b); that is

$$N_m=\bar{L}(1+\bar{L}^2/12-\bar{L}/2) \quad \text{for } m=0 \tag{25a}$$

$$N_m=\bar{L}[1+\bar{L}^2/(2m\pi)^2]/2 \quad \text{for } m=1,2,\ldots, \tag{25b}$$

Depending on when u_0 is positive or negative, the temperature solution at $x=0$ and $x=L$ are expected to behave differently. Because temperature depends on a large number of variables, typical values are selected for the sake of brevity. Data are obtained when $\tau_q=\tau_t$, $Sp=10$, and $\nu CL^2/k_e=10$ but for different $Pe=0$, 0.1, 0.2, 0.5, and 0.8. Fig. 6a shows the temperature of the solid and the liquid at $x=0$ when $Sp=10$, $\nu CL^2/k_e=10$, and $\bar{C}_{\mathrm{s}}/C=0.2$. Fig. 6b describes the temperature at the $x=L$ surface for the same parameters. When $u_0>0$, Fig. 6b shows that the temperature amplitude increases as *Pe* increases while there are negligible phase shifts for the extremums. The increase in temperature is due to an increase in the convective

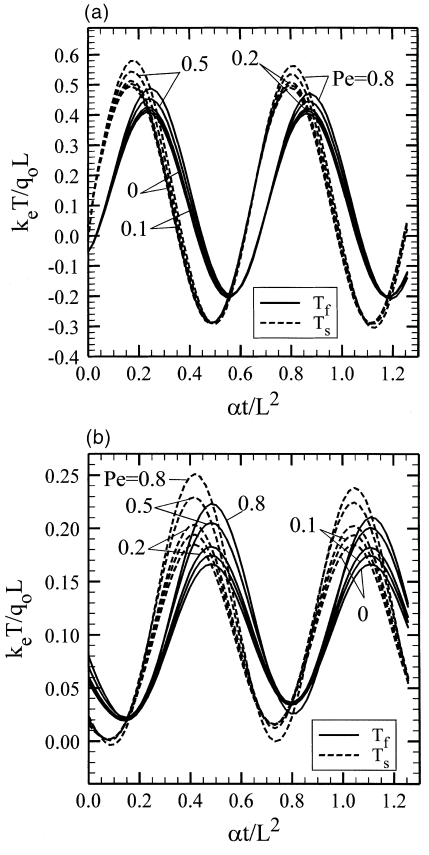

Fig. 6. (a) The effect of the Peclet number on fluid and solid temperature at $x=0$ when $q(0,\ t)=q_0\ \sin(\nu t)$, $Sp=10$, $u_0>0$, $\bar{C}=0.2$, $\tau_q=\tau_t$, and $\nu CL^2/k_e=10$. (b) The effect of the Peclet number on fluid and solid temperature at $x=L$ when $q(0,\ t)=q_0\ \sin(\nu t)$, $Sp=10$, $u_0>0$, $\bar{C}=0.2$, $\tau_q=\tau_t$, and $\nu CL^2/k_e=10$.

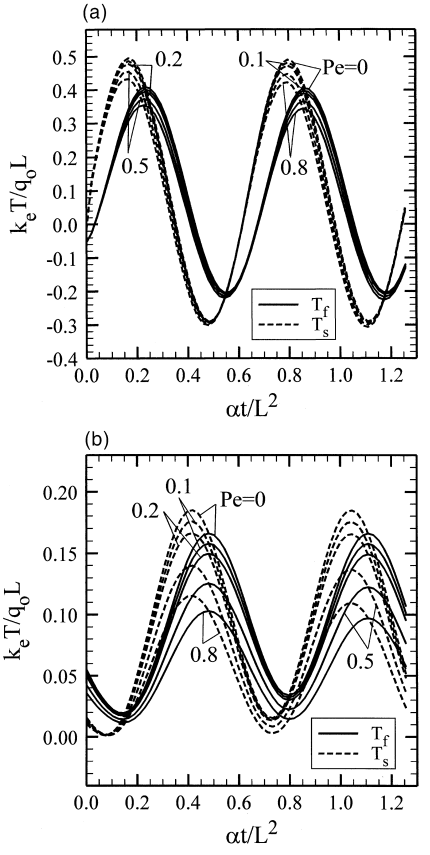

Fig. 7. (a) The effect of the Peclet number on fluid and solid temperature at $x=0$ when $q(0,\ t)=q_0\ \sin(\nu t)$, $Sp=10$, $u_0<0$, $\bar{C}=0.2$, $\tau_q=\tau_t$, and $\nu CL^2/k_e=10$. (b) The effect of the Peclet number on fluid and solid temperature at $x=L$ when $q(0,\ t)=q_0\ \sin(\nu t)$, $Sp=10$, $u_0<0$, $\bar{C}=0.2$, $\tau_q=\tau_t$, and $\nu CL^2/k_e=10$.

component of the energy transfer. This is demonstrated by reversing the direction of flow. The fluid and solid temperature are computed when velocity u_0 is opposite to the x-direction and using the same parameters as those in Figs. 6a and b. Figs. 7a and b show that this process will be reversed when $u_0<0$, that is, the temperature amplitude decreases as Pe increases.

To show the effect of higher frequency heat input values for this latter case, $u_0<0$, the phase angle and amplitude at $x=L$ are computed and plotted in Figs. 8a and b for $\bar{C}_s/C=0.2$. The solid lines in the figures are for $Sp=\infty$ and correspond to the condition of LTE while the dash lines and dot–dash lines are for $Sp=100$ and 10, respectively. The data show that the Pe has a profound effect on the phase angle at higher values of dimensionless frequency. Figs. 9a and b and 10a and b are prepared for $\bar{C}=0.5$ and 0.8, respectively. They clearly show some unexpected results for phase angle and amplitude at higher ranges of dimensionless frequency. The most notable one is a rapid drop in the phase angle for finite values at dimensionless frequency values larger than 50 when Pe is large and Sp is small. Based on this study, one should expect a larger departure from the local thermal equilibrium as $\tau_q\rightarrow 0$. A discussion concerning the expected value of τ_q is presented in the next section.

4. Remarks and discussions

The majority of studies concerning heat transfer in porous media are based on the local thermal equilibrium assumption. The study of nonequilibrium phenomena in porous media indicates that the assumption of local thermal equilibrium is not universally valid. In the presence of rapid surface heat input, the local thermal equilibrium fails to exist and large errors

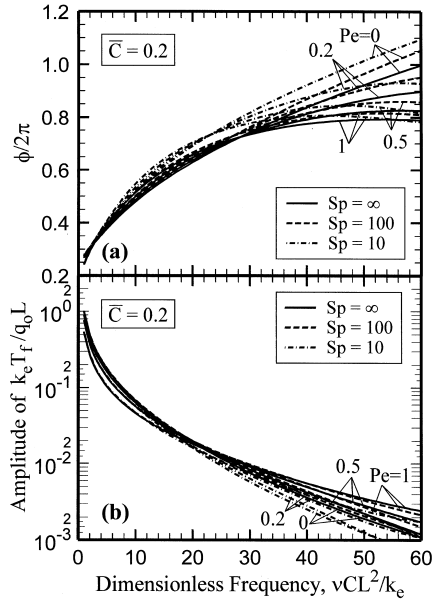

Fig. 8. The effect of the Peclet number on (a) the phase angle and (b) the amplitude for different Sparrow number at $x=L$ when $\bar{C}=0.2$ and $u_0<0$.

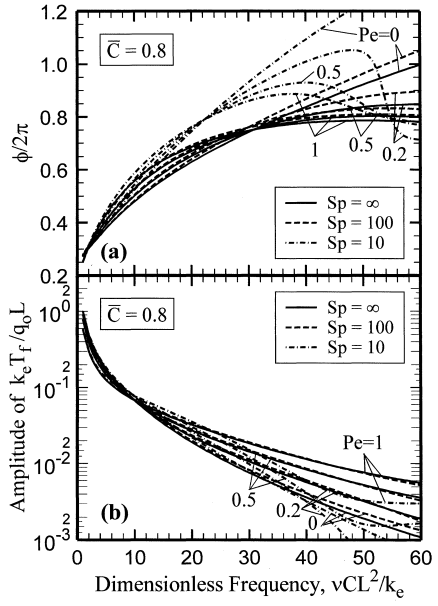

Fig. 10. The effect of the Peclet number on (a) the phase angle and (b) the amplitude for different Sparrow number at $x=L$ when $\bar{C}=0.8$ and $u_0<0$.

can be realized, depending on the value of the thermophysical properties. The value of the Sparrow number appears to be indicative of the presence of local thermal equilibrium for applications dealing with rapidly changing heat sources.

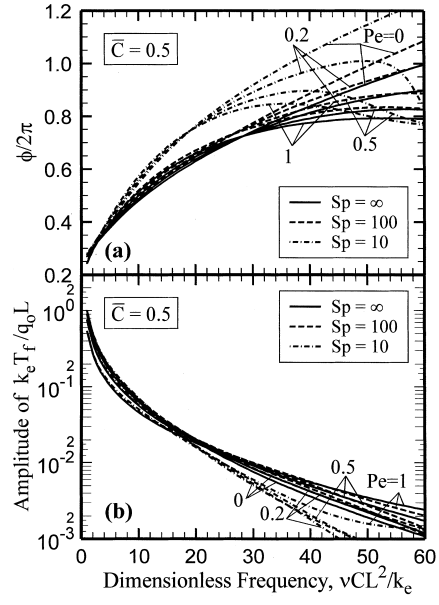

Fig. 9. The effect of the Peclet number on (a) the phase angle and (b) the amplitude for different Sparrow number at $x=L$ when $\bar{C}=0.5$ and $u_0<0$.

It is important to present a simple method of estimating the Sparrow number $hL^2/k_e r_h$. For no flow condition, one can show that the heat transfer is by natural convection. Since the Rayleigh number is generally small, the heat transfer is dominated by conduction and one can show that $Nu_{r_h}=hr_h/k_f$ is a constant. The value of the interstitial heat transfer h is constant for the no flow case. The value of h can be estimated based on the hypothesis that the mean solid temperature T_s and the mean fluid temperature T_f in a differential element are constant. If the Rayleigh number is small, the natural convection in a pore is dominated by conduction. The heat transfer coefficient is computed assuming a pore to have one of the following shapes: spherical, cylindrical prism, or square prism. The respective values $Nu_{r_h}=hr_p/k_f=1.09$, 1.45, or 1.23 show relatively small differences.

In general, the Sparrow number can be rewritten in terms of the Nusselt number as

$$Sp = Nu_{r_h}(k_f/k_e)(L/r_h)^2 \tag{26}$$

In the presence of a forced flow, $Nu_{r_h}=hr_h/k_f \approx 0.92$ is analogous to the Nusselt number for laminar flow in a circular passage. If the flow-passage profile, with a mean cross-section area A_c, is slightly different from circular, the empirical relation $Nu_{r_h}=0.92/[1+(A_c-4\pi r_h^2)/A_c]$ should provide an improved Nusselt number for that passage. Accordingly, Eq. (26) describes a simple method of estimating the Sparrow number; however, for an accurate estimate, the Sparrow num-

ber should be determined experimentally. Usually, $k_f < k_e$ and, according to Eq. (26), any value of $Sp \approx 10$ or less can be realized only if the thermal conductivity of the fluid is much smaller than k_e. The Sparrow number also provides an estimate of the lag time τ_t, that is

$$\frac{k_e \tau_t}{CL^2} = \frac{C_f/C}{Sp} \tag{27}$$

Another parameter that enters the analysis is τ_q. Experimental studies are needed to ascertain the proper value of τ_q. However, it is possible to provide an estimate of τ_q values using existing information in the literature. According to the Fourier equation, the heat flux across a control volume is related to ∇T. However, prior to onset of LTE, the actual heat flux is larger because thermal energy must be supplied to the individual structures within the control volume across contact surfaces and through constrictions. To account for the change in heat flux, one can set $\Delta A_s \Delta q \approx \Delta V_s C_s \, \partial(\Delta T_s)/\partial t$ where ΔT_s is the temperature difference across a contact surface. Substituting for $\Delta T_s = q R_c$ results in the relation

$$\Delta q = (\Delta V_s/\Delta A_s) C_s R_c (\partial q/\partial t) \tag{28}$$

where R_c is the contact resistance. A comparison with Eq. (6) suggests that $\tau_q \approx C_s R_c \Delta V_s/\Delta A_s$. The value of R_c depends on various factors including geometry, applied pressure, and the constriction effect; hence, it is difficult to develop an accurate prediction in the absence of experimental data.

The Sparrow number also controls the state of local thermal equilibrium under steady-state operation. One can consider a one-dimensional porous layer with thickness L and assume flow in the pores is similar to flow in small passages whose hydraulic radius is r_h. The energy balance applied to a fluid element in a passage yields

$$T_s - T_f = \frac{Pe}{Sp} \cdot \frac{\partial T_f}{\partial (x/L)} \tag{29}$$

For x/L of the order of 1, the Sp/Pe of more than 100 ensures that the local value of $T_s - T_f$ will be less than one percent of the temperature variation in the fluid. Therefore, Sp/Pe introduces a simple method of verifying the existence of LTE under a steady state operating condition.

5. Conclusion

Usually an estimate of the Sparrow number is sufficient to ascertain the state of the LTE condition. It is interesting to note that the heat transfer coefficient in a pore can be very large but the Nusselt number, as defined here, is nearly constant; ~1.0 for the conduction case and ~0.9 for incompressible laminar flow in the pores. Using these values, Eq. (26) provides a quick method of predicting the size of the Sp number. For the case of conduction, a large Sp number is indicative of the existence of LTE. However, in the presence of flow, the analysis presented here is valid only if Sp/Re is large. For a general case when LTE is absent, one should treat solid and liquid as two different systems [35–38].

The study presented here confirms that, in various situations, the commonly used assumption of local thermal equilibrium is satisfactory. However, in conjunction with studies in Vafai and Sozen [35,44], Amiri and Vafai [36,37], and Lee and Vafai [38], the assumption of local thermal equilibrium does fail in a substantial number of applications depending on the criteria specified in those studies. This work establishes one such area of failure corresponding to the presence of rapidly changing surface heat flux. In general, for rapidly changing heat sources, it is important to estimate the Sparrow number. A sufficiently large Sparrow number is indicative of the presence of a local thermal equilibrium condition.

References

[1] P. Cheng, W.J. Minkowycz, Free convection abut a vertical flat plate embedded in a saturated porous medium with application to heat transfer about a dike, Journal of Geophysical Research 82 (1977) 2040–2044.

[2] A.B. Kazanskiy, A.N. Zolotokrylin, Missing component in the equation for the land surface heat balance as applied to the heat exchange between the desert or semi-desert surface, Boundary-Layer Meteorology 71 (1994) 189–195.

[3] D.M. Manole, J.L. Lage, Numerical simulation of supercritical Hadley circulation within a porous layer, induced by inclined temperature gradients, International Journal of Heat and Mass Transfer 38 (1995) 2583–2593.

[4] R.M. Abalone, M.A. Lara, R. Gaspar, R.D. Piacentini, Drying of biological products with significant volume variations. Experimental and modeling results for potato drying, Drying Technology 12 (1994) 629–647.

[5] L. Zhang, P.J. Fryer, Models for the electrical heating of solid–liquid food mixtures, Chemical Engineering Science 48 (1993) 633–642.

[6] K.G.T. Hollands, K. Iynkaran, Analytical model for the thermal conductance of compound honeycomb transparent insulation, with experimental validation, Solar Energy 51 (1993) 223–227.

[7] J.R. Leith, A. Haji-Sheikh, A transient technique for finding effective thermal conductivity of fluid saturated porous media. Symposium on Heat Transfer in Porous

Media. Beck, Yao (Eds.), ASME HTD-Vol. 22, Bk. No. H00250 (1982) 93–101.
[8] J. Selih, A.C.M. Sousa, T.W. Bremner, Moisture and heat flow in concrete walls exposed to fire, Journal of Engineering Mechanics of ASCE 120 (1994) 2028–2043.
[9] L.W. Hrubesh, R.W. Pekala, Thermal properties of organic and inorganic aerogels, Journal of Materials Research 9 (1994) 731–738.
[10] A.I. van Heek, Increasing the power of the high temperature reactor module, Nuclear Engineering and Designs 150 (1994) 183–189.
[11] T.C. Chawla, D.R. Pedersen, W.J. Minkowycz, Governing equations for heat and mass transfer in heat generating porous beds. Part I: coolant boiling and transient void propagation, International Journal of Heat and Mass Transfer 28 (1985) 2129–2136.
[12] T.C. Chawla, D.R. Pedersen, W.J. Minkowycz, Governing equations for heat and mass transfer in heat generating porous beds. Part II: particulate melting and substrate penetration by dissolution, International Journal of Heat and Mass Transfer 28 (1985) 2137–3148.
[13] I. Catton, M. Chung, Two-phase flow in porous media with phase change: post dryout heat transfer and steam injection, Nuclear Engineering Designs 151 (1994) 185.
[14] K. Vafai, J. Ettefagh, Analysis of the radiative and conductive heat transfer characteristics of a waste package canister, ASME Journal of Heat Transfer 110 (1998) 1011–1014.
[15] M. Sözen, K. Vafai, L.A. Kennedy, Thermal charging and discharging of sensible and latent heat storage packed beds, Journal of Thermophysics and Heat Transfer 5 (1991) 623–625.
[16] M.S. Bohn, L.W. Swanson, A comparison of models and experimental data for pressure drop and heat transfer in irrigated packed beds, International Journal of Heat and Mass Transfer 34 (1991) 2509–2519.
[17] K.B. Lee, J.R. Howell, Theoretical and experimental heat and mass transfer in highly porous media, International Journal of Heat and Mass Transfer 34 (1991) 2123–2132.
[18] C.-K. Chen, C.-H. Chen, W.J. Minkowycz, U.S. Gill, Non-Darcian effects on mixed convection about a vertical cylinder embedded in a saturated porous medium, International Journal of Heat and Mass Transfer 35 (1992) 3041–3046.
[19] B.A. Masha, G.S. Beavers, E.M. Sparrow, Experiments on the resistance law for non-Darcy compressible gas flows in porous media, Journal of Fluids Engineering 96 (1974) 353–357.
[20] L.B. Younis, R. Viskanta, Experimental determination of the volumetric heat transfer coefficient between stream of air and ceramic foam, International Journal of Heat and Mass Transfer 36 (1993) 1425–1434.
[21] D. Getachew, D. Poulikakos, W.J. Minkowycz, Double diffusion in a porous cavity saturated with non-Newtonian fluid, Journal of Thermophysics and Heat Transfer 12 (1998) 437–446.
[22] K. Vafai, C.-L. Tien, Boundary and inertia effects on convective heat transfer in porous media, International Journal of Heat and Mass Transfer 34 (1981) 195–203.
[23] D. Getachew, W.J. Minkowycz, D. Poulikakos, Macroscopic equations of non-Newtonian fluid flow and heat transfer in a porous matrix, Journal of Porous Media 1 (1998) 273–283.
[24] E.M. Sparrow, G.S. Beavers, B.A. Masha, Laminar flow in a rectangular duct bounded by a porous wall, Physics of Fluids 17 (1974) 1465–1467.
[25] A. Bejan, K.R. Khair, Heat and mass transfer by natural convection in a porous medium, International Journal of Heat and Mass Transfer 28 (1985) 909–918.
[26] G.S. Beavers, A. Hajji, E.M. Sparrow, Fluid flow through a class of highly-deformable porous media Part 1: experiments with air, Journal of Fluids Engineering 103 (1981) 432–439.
[27] G.S. Beavers, K. Wittenberg, E.M. Sparrow, Fluid flow through a class of highly-deformable porous media Part II: experiments with water, Journal of Fluids Engineering 103 (1981) 440–444.
[28] M. Sozen, K. Vafai, Analysis of the non-thermal equilibrium condensing flow of a gas through a packed bed, International Journal of Heat and Mass Transfer 33 (1990) 1247–1261.
[29] P.C. Huang, K. Vafai, Passive alteration and control of convective heat transfer utilizing alternate porous cavity/block wafers, International Journal of Heat and Fluid Flow 15 (1994) 48–61.
[30] G.P. Peterson, C.S. Chang, Two-phase heat dissipation utilizing porous-channels of high-conductivity material, ASME Journal of Heat Transfer 120 (1998) 243–252.
[31] J. Bear, Dynamics of Fluids in Porous Media, Dover, New York, 1972.
[32] D.A. Nield, A. Bejan, Convection in Porous Media, Springer, New York, 1992.
[33] M. Kaviany, Principles of Heat Transfer in Porous Media, Springer-Verlag, New York, 1991.
[34] C.-L. Tien, K. Vafai, Convective and radiative heat transfer in porous media, Advances in Applied Mechanics 27 (1989) 225–282.
[35] K. Vafai, M. Sozen, Analysis of energy and momentum transport for fluid flow through a porous bed, ASME Journal of Heat Transfer 112 (1990) 690–699.
[36] A. Amiri, K. Vafai, Analysis of dispersion effects and non-thermal equilibrium, non-Darcian, variable porosity incompressible flow through porous media, International Journal of Heat and Mass Transfer 37 (1994) 939–954.
[37] A. Amiri, K. Vafai, Transient analysis of incompressible flow through a packed bed, International Journal of Heat and Mass Transfer 41 (1998) 4259–4279.
[38] D.Y. Lee, K. Vafai, Analytical characterization and conceptual assessment of solid and fluid temperature differentials in porous media, International Journal of Heat and Mass Transfer 42 (1999) 423–435.
[39] D. Fournier, A.C. Boccara, Heterogeneous media and rough surfaces: a fractal approach for heat diffusion studies, Physics (A) 157 (1989) 587–592.
[40] D.K. Tzou, Macro- to Microscale Heat Transfer, Taylor and Francis, New York, 1997.
[41] K.J. Hays-Stang, A. Haji-Sheikh, A unified solution for heat conduction in thin films, International Journal of Heat and Mass Transfer 42 (1999) 455–465.

[42] C.L. Tien, K. Vafai, Statistical bounds for the effective thermal conductivity of microsphere and fibrous insulation, AIAA Progress Series 65 (1979) 135–148.
[43] J.V. Beck, K.D. Cole, A. Haji-Sheikh, B. Litkouhi, Heat Conduction Using Green's functions, Hemisphere, Washington, DC, 1992.
[44] K. Vafai, M. Sozen, An investigation of a latent heat storage packed bed and condensing flow through it, ASME Journal of Heat Transfer 112 (1990) 1014–1022.